Seed-mediated Growth of Au Nanoplates on the Functionalized Reduced Graphene Oxide Films for Surface-enhanced Raman Scattering

Young-Kwan Kim,[†,*] Hongje Jang,[‡] and Kyungtae Kang[§]

[†]*Carbon Composite Materials Research Center, Institute of Advanced Composite Materials, Korea Institute of Science and Technology, San 101, Eunha-ri, Bongdong-eup, Wanju-gun, Jeollabuk-do 565-905, Korea. *E-mail: youngkwan@kist.re.kr*
[‡]*Department of Chemistry, Kwangwoon University, Seoul 139-701, Korea*
[§]*Department of Applied Chemistry, Kyung Hee University, Yongin 446-701, South Korea*
Received April 11, 2017, Accepted July 4, 2017, Published online August 24, 2017

We developed a seed-mediated growth strategy for the synthesis of Au nanoplate on the pyrene ethyleneglycol amine (PEA) functionalized reduced graphene oxide (PEA-RGO) films. This process yielded 17.6% of Au nanoplates on the PEA-RGO films, and the synthesized Au nanoplate/PEA-RGO nanohybrid films showed high potential as a surface-enhanced Raman scattering (SERS) platform.

Keywords: Au nanoplate, Graphene oxide, Surface-enhanced Raman scattering

Introduction

Graphene oxide (GO) has attracted much research interest due to its unique and excellent optochemical properties such as amphiphilic, chemically tailorable surface, fluorescence quenching, high-optical absorption in near infrared region, and Raman scattering.[1] In addition, GO can be converted into a graphene analog—reduced GO (RGO)—by chemical and/or thermal reduction processes, which lead to the partial restoration of sp^2 carbon networked structures.[2] The optochemical properties of GO and RGO depend considerably on their chemical structures[3] and hybridization with other functional nanomaterials.[4] Therefore, the syntheses of GO- and RGO-based nanohybrid structures have been extensively attempted to further enhance the optochemical properties of GO and RGO or to endow a new function to them.[4]

The GO and RGO-based structures hybridized with metallic nanoparticles (NPs) have been widely investigated for the applications to various research fields including catalysts,[5] photovoltaics,[6] optoelectrical devices,[7] theranostics,[8] and analytical platforms.[9] Especially, surface-enhanced Raman scattering (SERS) is one of the promising analytical techniques that can be coupled with nanohybrid structures composed of Au NPs and RGO, because these structures can enhance the Raman signals of probe molecules through electromagnetic and chemical enhancements.[10] In this regard, controlled synthesis of Au nanostructures on RGO is an important prerequisite, given that the SERS property of Au/RGO nanohybrid structures depends significantly on the shape and dimension of Au nanostructures grown on the RGO.[11]

Therefore, various Au nanostructures such as spheres, stars, and rods have been synthesized onto the RGO films and the resulting Au/RGO nanohybrid structures exhibited a great promise as an efficient SERS platform.[12–15] However, the synthesis of Au nanoplates on RGO has not been reported, despite the reported high electromagnetic field-enhancing property of Au nanoplates compared to Au nanospheres and nanorods.[16] Furthermore, surface-grown Au nanoplates are useful to develop sensing platforms, because they can be functionalized depending on its crystalline facet.[17] Many efforts have been devoted to the synthesis of Au nanoplates; one of the interesting approaches is a seed-mediated growth, in which the shape of Au nanostructures was reported to be controllable by the addition of halide ions to the typical solution consisting of Au seeds, ascorbic acid (AA), chloroauric acid, and cetyl trimethylammonium bromide (CTAB).[18] Based on this strategy, Au nanoplates were successfully prepared in the presence of iodide ions.

We previously reported that the seed-mediated growth strategy was successfully applied to the surface-immobilized Au seeds to synthesize Au nanorods and Au nanospheres directly on the functionalized RGO films.[19,20] The shape of synthesized Au nanostructures could be controlled by varying the surface chemistry of RGO films.[21] Herein, we investigated the seed-growth approach to synthesize Au nanoplates on the surfaces of RGO films by using strategies that we previously developed, with a proper modification of growing conditions—addition of potassium iodide (KI). The iodide ions can bind to the low-indexed Au crystalline facet and thus drastically change the reduction kinetics of $AuCl_4^-$ and CTAB complexes by AA depending on the crystalline facets that the Au nanocrystals are growing on.[18] By combining our seed-mediated surface growth strategy with the addition of iodide ions, Au

nanoplates were successfully grown on the surface of functionalized RGO films (Figure 1) and the resulting Au nanoplates/RGO films presented high applicability as a SERS platform.

Experimental

Materials. Natural graphite (FP 99.95 % pure) was purchased from Graphit Kropfmühl AG (Hauzenberg, Germany). Hydrogen tetrachloroaurate(III) hydrate was purchased from Kojima Chemicals Co.(Sayama, Saitama, Japan). CTAB and di-tert-butyl dicarbonate were purchased from Across (Geel, Belgium). Ethanol was purchased from Merck (Darmstadt, Germany). Sodium borohydride, AA, KI, diisopropylethylamine, 3-aminopropyltriethoxysilane (3-APTES), dicyclohexylcarbodimide, trifluoroacetic acid, pyrene butyric acid, 1-hydroxybenzotriazole, and 1,2-Bis(2-aminoethoxy)ethane were purchased from Aldrich Chemical Co. (Milwaukee, WI, USA). Trisodium citrate dehydrate and chloroform were purchased from Junsei Chemical Co. (Tokyo, Japan). Sulfuric acid and Potassium permanganate were purchased from Samchun (Seoul, Korea). Hydrogen peroxide, sodium nitrate, toluene and *N*,*N*-dimethylformamide (DMF) were purchased from Daejung chemical (Siheung, Korea). The 500-nm SiO_2/P^{++} Si substrates (500 μm in thickness) and 4 inch quartz wafers (500 μm in thickness) were respectively purchased from STC (Tokyo, Japan) and i-Nexus (Stamford, CT, USA). All chemicals were used as received.

Synthesis of GO. To a solution of 23 mL of H_2SO_4, 1.5 g of natural graphite, and 0.5 g of $NaNO_3$ were added and stirred in an ice bath. Then, 3 g of $KMnO_4$ was gradually added to the mixture with stirring while temperature was maintained below 20°C. After addition, the acid mixture was heated to 35°C and stirred for 1 h. Then, 40 mL of distilled water was added to the mixture and stirred for 30 min. About 100 mL of water was added to the reaction mixture in an ice bath to prevent rapid boiling of the acid mixture. Finally, 3 mL of H_2O_2 (30%) was dropped to the reaction mixture, this step cause color change from brown to yellow and evolution of bubbles. The mixture was centrifuged at 8000 rpm and washed three times with 3.5% HCl and water. The purified mixture was diluted with water to prepared stock solution of GO.

Synthesis of Au seeds. An aqueous solution (20 mL) of trisodium citrate (250 μM) and $HAuCl_4$ (250 μM) was prepared in round bottom flask. Then, 0.6 mL of ice cooled $NaBH_4$ solution (0.1 M) was added to the solution immediately with gentle shaking. The diameter of synthesized particles was approximately 5 nm. The Au nanoparticles were used as a seed for Au nanoplate growth after 6 h from synthesis.

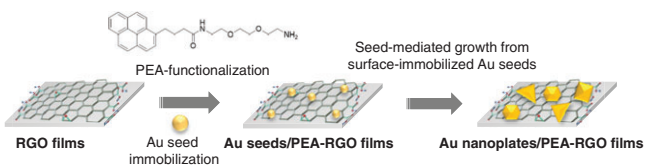

Figure 1. Scheme of the seed-mediated growth of Au nanoplates on the functionalized RGO films.

Immobilization of GO on the substrate. The 500-nm SiO_2/Si substrates were immersed in the piranha solution (hydrogen peroxide [30%]: sulfuric acid = 1:3, warning: piranha solution is highly corrosive and dangerous. Handle with caution.) for 10 min at 125°C, washed with water and ethanol and dried under a stream of nitrogen. The piranha treated substrates were immersed in the 10 mM toluene solution of 3-APTES for 30 min washed with water and ethanol and dried under a stream of nitrogen. After surface functionalization, the substrates were immersed in the GO suspension (1.0 mg/mL) for 1 h, washed with water and ethanol and dried under a stream of nitrogen. This process leads to the formation of GO films with high surface coverage.

Reduction of GO Films on the Substrate. The GO films coated substrates were immersed in the 20% hydrazine monohydrate solution in DMF at 80°C for 24 h, washed with water and ethanol and dried under a stream of nitrogen. The hydrazine treated substrates were further reduced by thermal annealing at 500°C for 1 h under nitrogen atmosphere. By this process, RGO films were successfully prepared.

Synthesis of Pyrene Ethyleneglycol Amine (PEA). PEA was synthesized our previous protocol and the detailed protocol was described in elsewhere.[19,21]

Seed-mediated Growth of Au Nanoplates on RGO Surface. The RGO films coated substrates were immersed in the 1 mM ethanolic solution of PEA for 12 h, washed with water and ethanol and dried under a stream of nitrogen. The surface functionalized RGO films were immersed in the prepared Au seed solution for 20 min, washed with water and ethanol and dried under a stream of nitrogen. The seeded RGO films were immersed in the growing solution containing 9 mL of 0.1 M CTAB, 1 mL of 2.5 mM $HAuCl_4$, 200 μL of 0.1 M ascorbic acid, and 20 μL of 20 mM KI for 1 h, washed with water and ethanol and dried under a stream of nitrogen.

Characterization. Size of Au seeds was determined by Tecnai G2 F30 Field Emission TEM (FEI company, Eindhoven, The Netherlands). S-4800 Field emission SEM (Hitachi, Tokyo, Japan) was used to observe heterogeneous interfacing system of RGO and Au nanoplates on SiO_2/Si substrates. AFM image and profile of GO were taken with an XE-100 (Park system, Suwon, Korea) with a backside gold coated silicon probe (M to N, Yongin, Korea). Raman spectra of the GO, RGO, and heterogeneous interfacing system of RGO and Au nanoplates on SiO_2/Si substrates were obtained by HORIBA LabRAM (jobin Yvon, Palaiseau, France) using an air-cooled He/Ne laser (632.8 nm) as an excitation source focused through an integral microscope (Olympus BX 41, Olympus, Tokyo, Japan). Raman scattering signal was detected with 180° geometry using

and air-cooled 1024 × 256 pixel CCD detector. The UV–Vis spectra were recorded with a UV-2550 (Shimadzu, Kyoto, Japan) using quartz substrate. FT-IR spectrum of GO was obtained with an EQUINOX55 (Bruker, Rheinstetten, Germany) using the KBr pellet method. Ellipsometric analysis was carried out with a L116S (Gaertner Scientific Coporation, Skokie, IL, USA)

Results and Discussion

We first synthesized GO by using the Hummers's method and dispersed it in distilled water by sonication for single layer exfoliation. The lateral dimension of GO sheets lied within a broad range from few hundreds of nanometer to micrometer with thickness corresponding to the single layer (0.87 nm) (Figure 2(a) and (b)). UV–Vis spectrum of GO showed typical p–p* and n–p* transitions of GO around 230 and 300 nm (Figure 2(c)). FT-IR spectrum of GO also exhibited several characteristic peaks originated from oxygen containing functional groups such as alcohol at 3415 and 1400 cm^{-1} from O–H vibration and deformation, carboxylic acid at 1716 cm^{-1} from C=O stretching and epoxy at 1079 cm^{-1} from C–O stretching (Figure 2(d)). These results clearly confirmed the successful synthesis of GO.

Then, the GO was immobilized on the surface of Si substrates functionalized with 3-APTES by simply immersing the substrates into the GO suspension.[22] The resultant GO films were thermally baked to stabilize the interface between the GO and substrates, and then reduced in a DMF solution of hydrazine monohydrate. The prepared RGO films showed high surface coverages on the substrates (Figure 3(a)) and had a thickness of 0.97 nm, which corresponds to a single-layered graphene (Figure 3(b)). The structural changes of GO films during the reduction were examined by UV–Vis and Raman spectroscopic analyses. UV–Vis spectrum of RGO films revealed the red-shifted

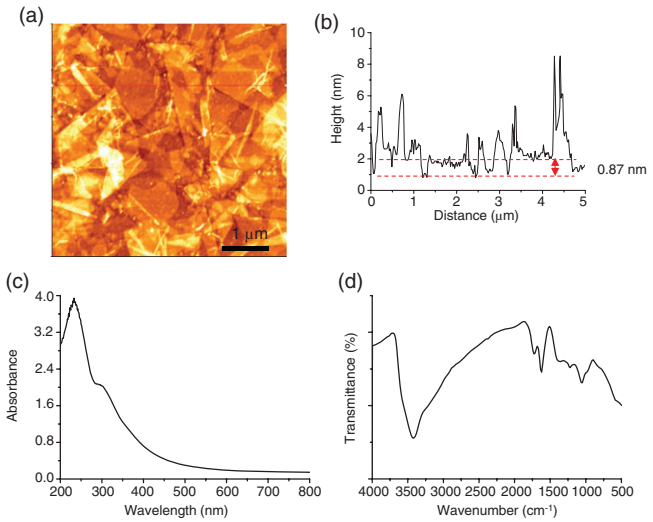

Figure 2. (a) AFM image, (b) line profile, (c) UV–Vis, and (d) FT-IR spectrum of GO.

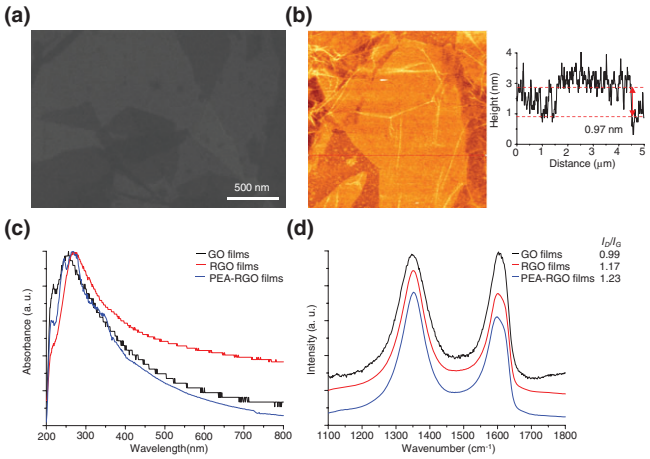

Figure 3. (a) Scanning electron microscopy (SEM) and (b) atomic force microscopy (AFM) images of prepared GO with line profile. (c) UV–Vis and (d) Raman spectra of GO, RGO, and PEA-RGO films.

π–π* transition peak from 256 nm (GO films) to 268 nm (Figure 3(c)). The Raman spectrum of RGO films also exhibited the increased intensity ratio of D- and G-peaks (I_D/I_G) from 0.98 (GO films) to 1.17 (Figure 3(d)). These changes implied the successful conversion of GO into RGO films.[22] The RGO films were then immersed into an ethanolic solution of PEA to introduce primary amine groups on the surface of RGO films.[19,21] The successful functionalization with PEA was confirmed by the appearance of its typical absorption peaks at 244, 268, 279, 332, and 349 nm (Figure 3(c)) and increased I_D/I_G, which reflected the strong interaction between PEA and RGO films.[19,21]

The PEA-functionalized RGO (PEA-RGO) films were immersed in a suspension of Au nanoparticles (Au seeds) to immobilize the Au seeds on the prepared film surfaces.[19,21] The Au seeds loaded PEA-RGO (Au seeds/PEA-RGO) films were then incubated in a growing solution containing 9 mL of 0.1 M CTAB, 1 mL of 2.5 mM $HAuCl_4$, 200 μL of 0.1 M AA, and 20 μL of 20 mM KI for 1 h, for the seed-mediated growth of Au nanoplates. This seed-mediated growth process resulted in the synthesis of Au nanoplates attached on the Au seeds/PEA-RGO films.

SEM images showed the morphologies of Au nanostructures grown on Au seeds/PEA-RGO films (Figure 4(a) and (b)). Au nanoplates and polygonal nanoparticles coexisted on the Au seeds/PEA-RGO films. The yield of the Au nanoplates was about 17.6% calculated from the SEM images by dividing the number of Au nanoplates with total number of gold nanostructures. This yield is considerably higher than that of Au nanorods grown by the similar seed-mediated growth strategy.[19] According to the SEM analysis of grown Au nanoplates, the edge length distribution was mainly observed in the range of 200–300 nm (Figure 4(a) and (b)). The thickness of Ag nanoplates was approximately measured as 11 nm (Figure 4(c)). For those with increased edge length, the tips of triangular Au nanoplates were more truncated

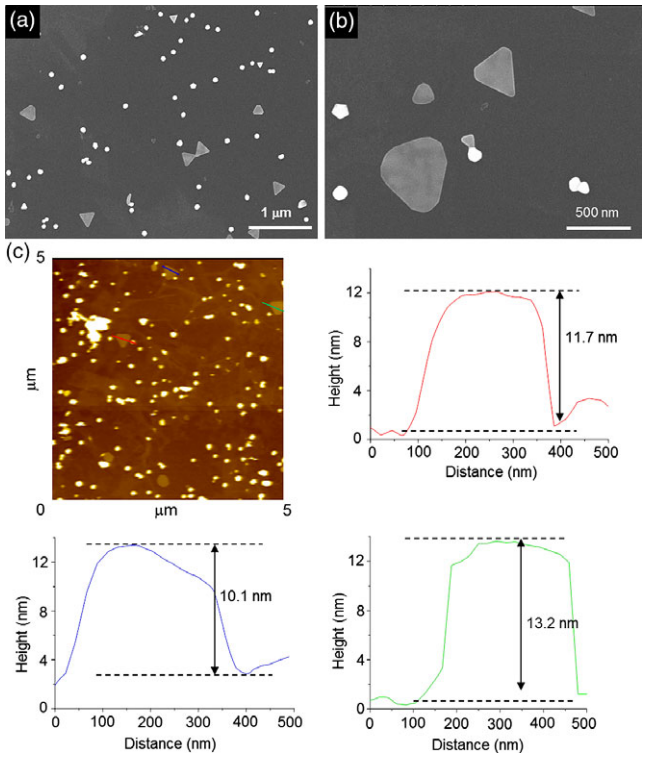

Figure 4. (a and b) SEM images of Au nanoplates/PEA-RGO films with different magnification. (c) AFM image and line profiles of Au nanoplates/PEA-RGO films.

(Figure 4(b)). This tendency was generally observed in the seed-mediated growth of metal nanoplates.[23]

The growth of Au nanoplates was also confirmed by the appearance of a typical localized surface plasmon resonance (LSPR) band of Au nanostructures at 540 nm that originated from the dipole resonance of polygonal Au nanoparticles and in-plane dipole resonance of Au nanoplates, whereas the Au seeds/PEA-RGO films presented negligible LSPR bands and broadened peaks of PEA at 244 and 349 nm (Figure 5(a)). Because of the LSPR effect from Au nanoplates, Raman spectrum of Au nanoplates-grown PEA-RGO (Au nanoplates/PEA-RGO) films showed 3.9- and 5-fold augmented D- and G-peaks, respectively, in comparison with Raman spectrum of normal RGO films (Figure 5(b)). The applicability of Au nanoplates/PEA-RGO films as a SERS platform was examined by using a conventional Raman probe, Rhodamine 6G (R6G). RGO and Au nanoplates/PEA-RGO films were treated by 100 pmol of R6G and analyzed by Raman spectroscopy. An SERS spectrum of R6G on Au nanoplates/PEA-RGO films clearly exhibited the characteristic peaks at 1309, 1360, 1418, 1506, 1572, and 1648 cm^{-1} (Figure 5(c)).[23] By contrast, only two broad peaks around 1360 and 1572 cm^{-1} were observed on RGO films. In addition, the Raman signal of R6G at 1572 cm^{-1} was 4-fold enhanced on Au nanoplates/PEA-RGO compared to RGO films. This result supported that the Au nanoplates/PEA-RGO films can be utilized as a SERS platform to develop a SERS-based chemical- and bio-sensors, harnessing the tailorable surface properties of Au nanoplates.

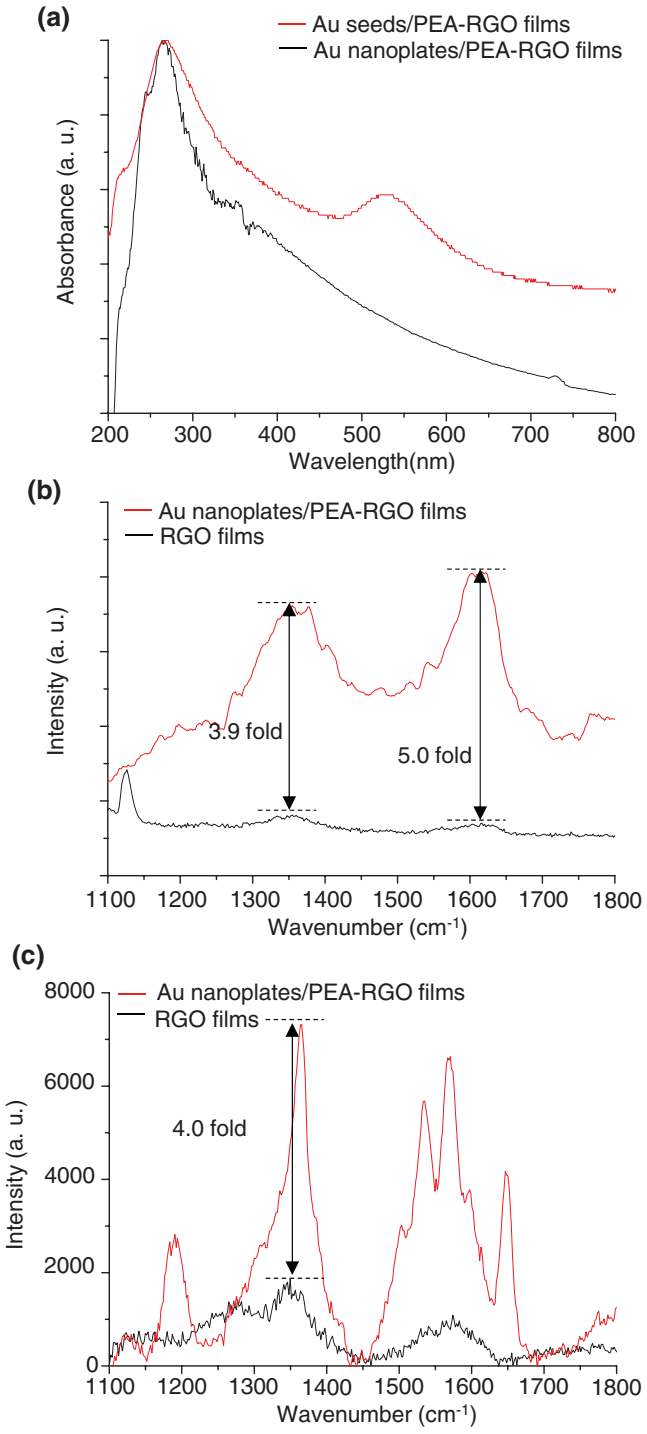

Figure 5. (a) UV–Vis and (b) Raman spectra of Au seeds/PEA-RGO and Au nanoplates/PEA-RGO films. (c) SERS spectra of R6G obtained on RGO and Au nanoplates/PEA-RGO films with 514 nm excitation source. The Raman signals were normalized with a peak of Si at 990 cm^{-1}.

Conclusion

In conclusion, a seed-mediated synthetic strategy for the Au nanoplates on the functionalized RGO films was successfully demonstrated by adopting the solution phase Au

nanoplate synthesis approach with using halide ion to two-dimensional film surface. The synthesized Au nanoplates were strongly interacted with RGO films and thus significantly enhanced Raman signals from the underneath RGO films by their LSPR effect. Based on their LSPR effect, the Au nanoplates/PEA-RGO films presented considerably higher efficiency when used as a SERS platform than RGO films. We believe that this strategy will be an important and practical tool for the development of SERS-based advanced analytical platforms.

Acknowledgments. This research was financially supported by grants from the Korea Institute of Science and Technology (KIST) Open Research Program (ORP) and Nano · Material Technology Development Program through the National Research Foundation of Korea (NRF) funded by the Ministry of Science, ICT and Future Planning (2016M3A7B4027223, 2016M3A7B4905609). This work was also supported by NRF funded by Korean government (Grant Nos. NRF-2016R1C1B1008090).

References

1. K. P. Loh, Q. Bao, G. Eda, M. Chhowalla, *Nat. Chem.* **2010**, *2*, 1015.
2. D. R. Dreyer, S. Park, C. W. Bielawski, R. S. Ruoff, *Chem. Soc. Rev.* **2010**, *39*, 228.
3. Y.-K. Kim, D.-H. Min, *Chem. Euro. J.* **2015**, *21*, 7217.
4. X. Huang, Z. Yin, S. Wu, X. Qi, Q. He, Q. Zhang, Q. Yan, F. Boey, H. Zhang, *Small* **2011**, *7*, 1876.
5. J. S. Li, Y. Wang, C. H. Liu, S. L. Li, Y. G. Wang, L. Z. Dong, Z. H. Dai, Y. F. Li, Y. Q. Lan, *Nat. Commun.* **2016**, *7*, 11204.
6. G. S. Han, Y. H. Song, Y. U. Jin, J. W. Lee, N. G. Park, B. K. Kang, J. K. Lee, I. S. Cho, D. H. Yoon, H. S. Jung, *ACS App. Mater. Interfaces* **2015**, *7*, 23521.
7. X. Zeng, W. Tu, J. Li, J. Bao, Z. Dai, *ACS Appl. Mater. Interfaces* **2014**, *6*, 16197.
8. Y. Wang, L. Polavarapu, L. M. Liz-Marzán, *ACS Appl. Mater. Interfaces* **2014**, *6*, 21798.
9. J. H. Luong, S. K. Vashist, *Biosens. Bioelectron.* **2017**, *89*, 293.
10. M. Banchelli, B. Tiribilli, M. de Angelis, R. Pini, G. Caminati, P. Matteini, *ACS Appl. Mater. Interfaces* **2016**, *8*, 2628.
11. J. Huang, L. Zhang, B. Chen, N. Ji, F. Chen, Y. Zhang, Z. Zhang, *Nanoscale* **2010**, *2*, 2733.
12. P. Zhang, Y. Huang, X. Lu, S. Zhang, J. Li, G. Wei, Z. Su, *Langmuir* **2014**, *30*, 8980.
13. G. Jalani, M. Cerruti, *Nanoscale* **2015**, *7*, 9990.
14. T. H. Nguyen, Z. Zhang, A. Mustapha, H. Li, M. Lin, *J. Agric. Food Chem.* **2014**, *62*, 10445.
15. J. Y. Lee, Y. H. Park, A. K. Roy, B. Park, J.-H. Jang, S. Y. Park, I. In, *Chem. Lett.* **2015**, *44*, 665.
16. H. Wei, H. Xu, *Nanoscale* **2013**, *5*, 10794.
17. S. R. Beeram, F. P. Zamborini, *J. Am. Chem. Soc.* **2009**, *131*, 11689.
18. T. H. Ha, H.-J. Koo, B. H. Chung, *J. Phys. Chem. C* **2007**, *111*, 1123.
19. Y.-K. Kim, H.-K. Na, Y. W. Lee, H. Jang, S. W. Han, D.-H. Min, *Chem. Commun.* **2010**, *46*, 3185.
20. Y.-K. Kim, D.-H. Min, *Langmuir* **2012**, *28*, 4453.
21. Y.-K. Kim, H.-K. Na, D.-H. Min, *Langmuir* **2010**, *26*, 13065.
22. Y.-K. Kim, D.-H. Min, *Carbon Lett.* **2012**, *13*, 29.
23. Y.-K. Kim, D.-H. Min, *RSC Adv.* **2014**, *4*, 6950.

